Transition to superfluid turbulence in two-fluid flow of He II

Samuel Scott Courts and J. T. Tough
Department of Physics, The Ohio State University, Columbus, Ohio 43210
(Received 18 December 1987)

We have extended our previous measurements of the transition to superfluid turbulence in flows where the superfluid and normal-fluid velocities can be varied independently. The results indicate that the critical line in the V_n-V_s plane which forms the boundary between laminar flow and superfluid turbulence is a closed curve about the origin. The existence of this critical line suggests that most theories of the critical velocity in He II are incomplete.

INTRODUCTION

Liquid He II is described on the phenomenological level as a mixture of a normal-fluid component and a superfluid. The flow of He II in a tube can evidence a kind of dissipation associated with superfluid turbulence.[1] This turbulence is known to consist of a random tangle of quantized vortex lines in the superfluid. Schwarz[2] has been able to simulate the properties of a homogeneous tangle of vortex lines on a computer and finds good agreement with experiments done in pure superflow[3] (where the normal fluid is immobilized). Superfluid turbulence can be produced in many other types of flow where the normal fluid and superfluid have average speeds V_n and V_s. Some experiments of this type have been reported,[4-10] but many properties of this more general superfluid turbulence are still under investigation. In this paper we give experimental results for the onset of superfluid turbulence in flows where V_n and V_s can be varied independently. We compare our data with those of Marees and van Beelen.[8,9] The results indicate that there is a *critical line* in the V_n-V_s plane which separates superfluid turbulent flow from laminar flow. This critical line forms a closed curve about the origin, and the shape of this curve depends on the temperature of the He II. Our previous data,[11] confined to a small region of the V_n-V_s plane, had suggested the critical line was straight and independent of temperature. The present experiments clearly show that superfluid turbulence and "critical velocities" must be regarded as two-fluid phenomena.

APPARATUS

The transition from laminar flow to superfluid turbulence is determined in this experiment by observing the onset of the excess dissipation resulting from the turbulence. The experiment requires a well-characterized flow tube, a method for producing and measuring independent superfluid and normal-fluid velocities, and a sensitive measurement of the dissipation. Our experimental apparatus shown in Fig. 1 is a minor modification of that used previously.[11] A flow tube connects a large helium reservoir regulated at temperature T_1 to a small lower chamber containing a heater H_2. This chamber in turn is connected to a small upper chamber via a superleak. The superleak offers no resistance to the flow of superfluid but is impermeable to the flow of normal fluid. A bundle of fiberglass fibers wrapped on a heater H_1 is used to siphon superfluid from the main bath through the superleak and through the flow tube into the reservoir. We will call this device a film-flow transfer apparatus (FFTA).

The flow tube used in the experiment is the same one used previously. It is glass strengthened by a fiberglass sheath and coated with Stycast-1266 epoxy resin. The tube is 9.9 cm long (l) and the diameter of the tube (d) was determined to be 1.34×10^{-2} cm. After an extensive set of measurements was obtained for this flow tube the apparatus was warmed to room temperature, the inner surface of the tube was "roughened," and a second set of measurements was obtained. The roughening was produced by plating the inner tube surface with 1 μm diameter polystyrene spheres.[12] These spheres were suspended in methyl alcohol and drawn into the flow tube via capillary action. The polystyrene spheres remained fixed to the wall of the flow tube after the alcohol evaporated. Examination of the surfaces of sample flow tubes with a scanning electron microscope showed that the spheres tend to clump together in islands of about 25 spheres with a typical distance between islands of about 25 μm. Further investigation with the sample flow tubes showed that the spheres do not detach from the flow-tube wall after it has been cooled to liquid-nitrogen temperature.

Independently varied superfluid and normal-fluid velocities through the flow tube were produced by a combination of counterflow and superfluid transfer from the main bath. In pure counterflow, if $\dot{Q}$ is the power dissipated in H_2, then the two-fluid model yields an average normal-fluid velocity V_n towards the reservoir of

$$V_n=\dot{Q}/\rho STA\ , \tag{1}$$

where ρ is the He II density, S the specific entropy, T the average temperature, and A the area of the flow tube. The requirement in counterflow, that there be no net mass flow, results in a superfluid velocity $V_{s\mathrm{CF}}$ given by

$$V_{s\mathrm{CF}}=-V_n\rho_n/\rho_s\ , \tag{2}$$

where ρ_n and ρ_s are the normal and superfluid densities,

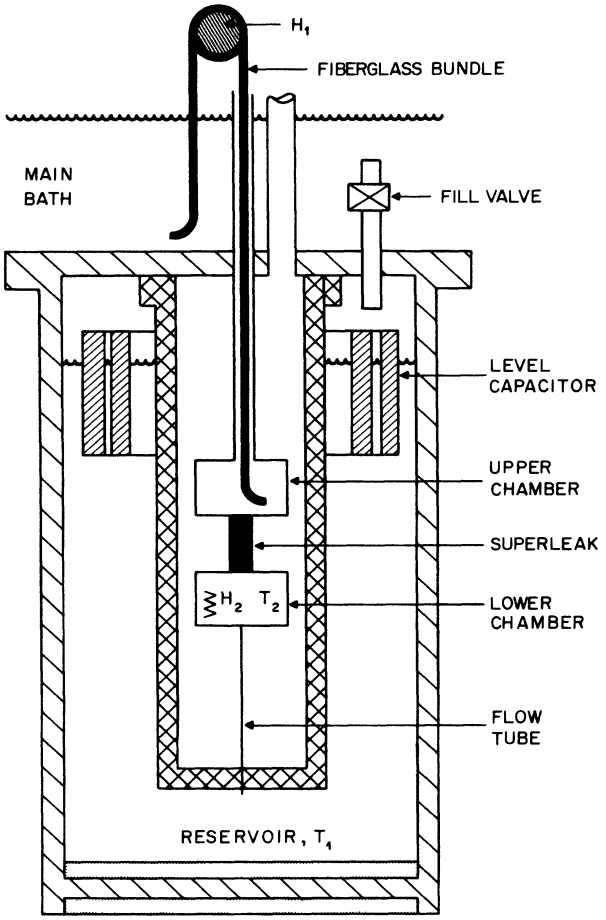

FIG. 1. Details of the experimental apparatus.

respectively, and V_{sCF} is the superfluid velocity due only to counterflow.

Pure superflow through the tube was produced by the FFTA. Superfluid helium film is siphoned over the fiberglass bundle from the main bath, over the heater H_1, and finally into the upper chamber. The heater H_1 acts as a control valve by increasing the local temperature of the helium film. The sensitivity of film flow to changes in temperature[13] results in very fine control of the superfluid transfer rate. The superfluid velocity through the flow tube due to the FFTA alone is labeled V_{sm}, i.e., this velocity results from a net mass transfer of superfluid into the reservoir can.

An order of magnitude estimate of V_{sm} can be obtained using the film-flow rate R over clean glass. At 1.5 K (Ref. 13)

$$R\ (\mathrm{cm^3/s}) = 0.75\times 10^{-4}\ (\mathrm{cm^3/cm\ s})\times P\ , \tag{3}$$

where P is the minimum perimeter over which the film flows. In the FFTA the minimum perimeter is the total perimeter of the fiberglass fibers in the bundle. The bundle consists of 7200 fibers of approximately 10^{-3} cm diameter (compared with a film thickness of about 10^{-6} cm). The minimum perimeter is then roughly $P=22$ cm which yields a transfer rate $R=1.7\times 10^{-3}$ cm^3/s. If the flow tube area is A, then V_{sm} is given by $V_{sm}=R/A=13$ cm/s. The highest value of V_{sm} seen in our experiment is about 40 cm/s. This is consistent with a film transfer rate of about $3R$ over the fiberglass, a value more typical of a rough metal surface.

The actual superfluid velocity due to the FFTA is determined from the rate of change of the level in the reservoir as superfluid was transferred from the bath. A cylindrical level-sensing capacitor was monitored with a General Radio 1615 capacitance bridge connected to an Ithaco 393 lock-in amplifier. A small computer was programmed to calculate the superfluid velocity after reading the output from the lock-in for up to 5 min. The lock-in output was also connected to a Hewlett-Packard 7044A X-Y chart recorder to preserve time records of the reservoir level. Estimates of sources of error in the calculation of V_{sm} indicate a maximum systematic error of 5% and a maximum random error of 0.06 cm/s. The total superfluid velocity through the flow tube V_s is the sum of the counterflow induced component V_{sCF} and the mass flow component V_{sm},

$$V_s = V_{sm} + V_{sCF}\ . \tag{4}$$

The temperature T_2 in the lower chamber was measured with a CG500 carbon glass resistor.[14] At $T=1.4$ K this device had a resistance of roughly 240 kΩ and a sensitivity $dR/RdT=5.48$ K^{-1}. The sensitivity was extremely stable and the resistance drift was on the order of 1 Ω per hour. This resistor was monitored with an SHE 120 resistance bridge with an excitation voltage set for maximum sensitivity with minimum self heating. The reservoir temperature T_1 was regulated electronically using standard techniques. Fluctuations in this regulated temperature were less than about 5 μK when averaged over 3 s.

PROCEDURE

Our experimental procedure consisted of measuring the temperature difference across the flow tube $\Delta T=T_2-T_1$ as a function of the two velocities V_n and V_s. Figure 2 shows a simplified diagram of our apparatus with the FFTA represented as a controlled current source. Figure 3 shows the region of the V_n-V_s plane accessible to our apparatus.

In pure counterflow, the superfluid current source is turned off so that $V_{sm}=0$ and $V_s=V_{sCF}$ [Eq. (4)]. Increasing the power $\dot{Q}$ in the heater H_2 increases V_n [Eq. (1)] and the trajectory given by the Eq. (2) is followed in the V_n-V_s plane. By adjusting the heater H_1, the superfluid current source can be controlled to give values of V_{sm} ranging from 0 to 25 cm/s. Appropriate combinations of counterflow and superflow can then provide access to the region of the V_n-V_s plane shown in Fig. 3.

In day to day operation one of two methods would be followed in taking data. In the first method, the value of the normal fluid velocity V_n would be set at some fixed value using heater H_2. A large superfluid velocity V_{sm} would then be added by means of the FFTA. The superfluid velocity V_{sm} would then be reduced in steps.

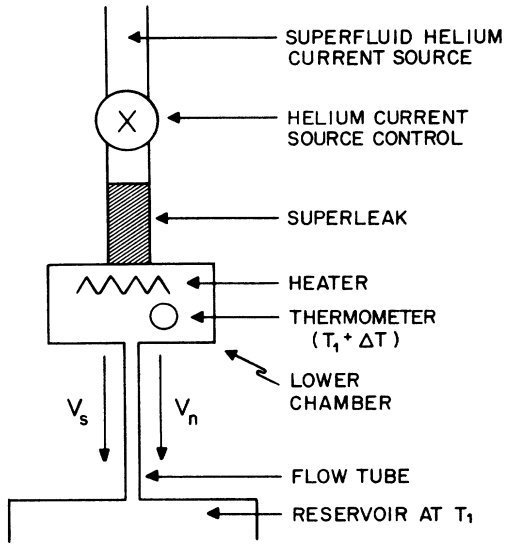

FIG. 2. Schematic diagram of the apparatus showing the directions of the normal and superfluid flow for the first quadrant of the V_n-V_s plane (positive V_n and positive V_s).

At each step the temperature T_2 would be monitored until a steady state was reached and ΔT was recorded. Beginning with a large V_{sm} insured that superfluid turbulence was generated in the flow tube. Steady state measurements of this type thus follow the vertical trajectories in Fig. 3. In a second method, the superfluid velocity V_{sm}, due to the FFTA, was held constant. The normal fluid velocity V_n, and superfluid velocity induced by counterflow V_{sCF}, were varied by controlling the power dissipated in H_2. The temperature difference was then

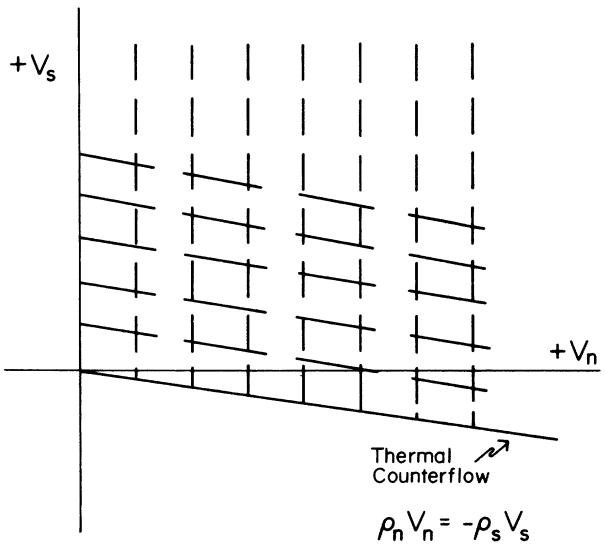

FIG. 3. First and fourth quadrants of the V_n-V_s plane showing the thermal counterflow trajectory (solid line) and the two types of experimental trajectories (dashed lines).

measured in steps yielding trajectories as shown in Fig. 3 parallel to the thermal counterflow line. This procedure was more difficult to follow and so only a limited amount of data was taken this way.

DATA

Measurements of the temperature difference ΔT, as a function of V_n and V_s, were taken at reservoir temperatures of 1.4, 1.6, and 1.8 K. At 1.4 K we followed vertical trajectories of $V_n=0$, 1, 2, 3, 4, 5, and 6 cm/s. Data taken in trajectories parallel to the counterflow line were taken at $V_{sm}=0$, 2.25, 3, and 4.5 cm/s. At 1.6 K we followed vertical trajectories of $V_n=0$, 0.5, 1, 1.5, 2, 2.75, 3.25, 3.75, and 4.8 cm/s. Trajectories parallel to the counterflow line were taken at $V_{sm}=0$, 0.8, 2, 3, and 4 cm/s. At 1.8 we followed vertical trajectories of $V_n=0$, 1, 2, and 3.5 cm/s. Trajectories parallel to the counterflow line were taken at $V_{sm}=2$, 3, and 4 cm/s. A second set of data was taken at $T=1.4$ K with the tube walls "roughened" to study the effect of surface roughness on the transition to superfluid turbulence. These data were taken in vertical trajectories of $V_n=0$, 2, 3, and 4 cm/sec and with trajectories parallel to the counterflow line at $V_{sm}=0$ and 3 cm/s.

The total temperature difference can be written as the sum of a viscous term ΔT_η, and a mutual friction term $\Delta T'$, due to the superfluid turbulence[1]

$$\Delta T=\Delta T_\eta+\Delta T' . \tag{5}$$

The viscous term is small, and is proportional to the normal fluid viscosity η, and the heat current $\dot{Q}$,

$$\Delta T_\eta=128\eta l\dot{Q}/(\rho S)^2 T\pi d^4 . \tag{6}$$

Equation (6) is used to compute ΔT_η, and the excess temperature difference $\Delta T'$ is then obtained from the ΔT data and Eq. (5).

Figure 4 shows a typical run taken using the first method. These data were taken at 1.6 K in a vertical trajectory with $V_n=2.75$ cm/s. (This trajectory is shown as the dashed line in Fig. 7.) Figure 4 is a plot of the excess temperature difference $\Delta T'$ as a function of V_s. As V_s is reduced from about 6 cm/s, $\Delta T'$ decreases sharply becoming zero below $V_s=3.9$ cm/s. Since the form of the dissipation is not known here, we simply take the transition from superfluid turbulence to laminar flow to occur at $V_s=(4.15\pm0.25)$ cm/s. In the laminar region where $\Delta T'=0$, there is no excess dissipation due to turbulence. The point $V_n=2.75$ cm/s and $V_s=4.15$ cm/s then denotes part of the boundary in the V_n-V_s plane separating a laminar region from superfluid turbulence.

Figure 5 shows a typical run taken using the second method. These data were taken at 1.8 K in a trajectory parallel to the thermal counterflow line with $V_{sm}=4.0$ cm/s. (This trajectory is shown as a dashed line in Fig. 8.) In the region between $V_n=1.0$ cm/s and $V_n=4.0$ cm/s there is no excess dissipation. There are two transitions to superfluid turbulence along this trajectory which occur at $V_n=(0.75\pm0.25)$ cm/s and $V_n=(4.25\pm0.25)$ cm/s, respectively. Therefore, the points $V_n=0.75$ cm/s,

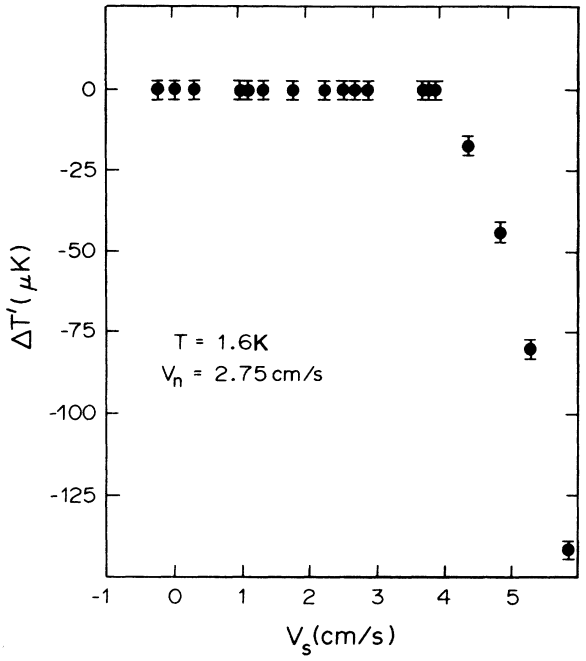

FIG. 4. The excess dissipation $\Delta T'$ as a function of V_s for fixed $V_n = 2.75$ cm/s at $T = 1.6$ K. The transition to superfluid turbulence occurs at $V_s = (4.15 \pm .25)$ cm/s. The trajectory for these data in the V_n-V_s plane is shown by the dashed line in Fig. 7.

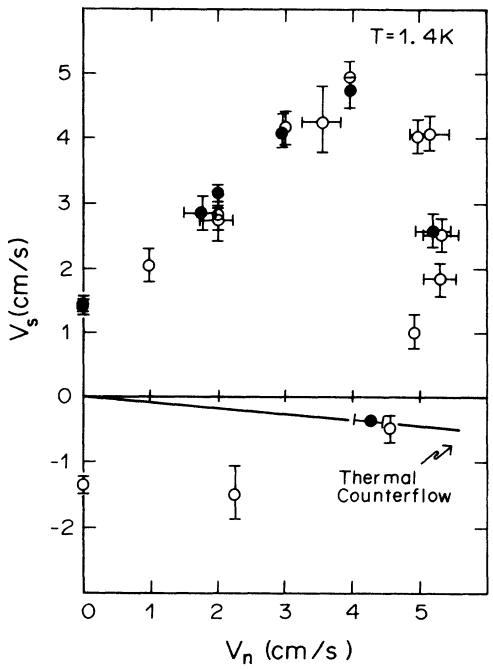

FIG. 6. The boundary of superfluid turbulence in the V_n-V_s plane at 1.4 K. The data points mark the transition between superfluid turbulence and laminar flow and fall on a critical line surrounding the origin. Points below the thermal counterflow line are from our previous results (Ref. 11). Solid symbols are results obtained with the artificially roughened flow tube.

$V_{sm} = 4$ cm/s ($V_s = 3.65$ cm/s), and $V_n = 4.25$ cm/s, $V_{sm} = 4$ cm/s ($V_s = 1.93$ cm/s) also lie on the boundary separating laminar flow from superfluid turbulence.

Figures 6–8 show the collection of these boundary points at the three temperatures studied. Points shown below the thermal counterflow line were obtained previ-

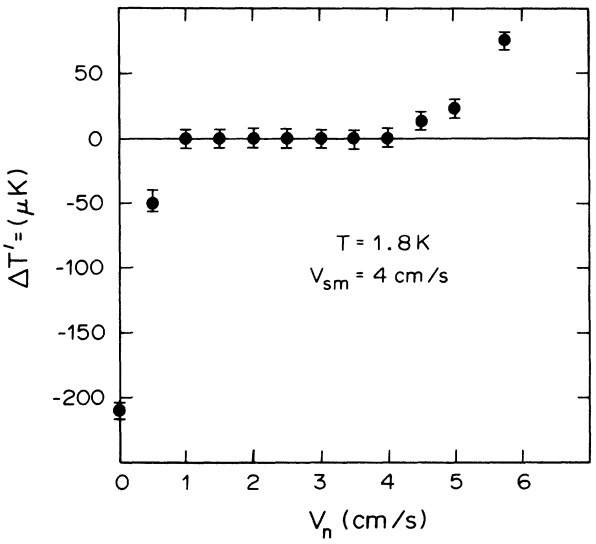

Fig. 5. The excess dissipation $\Delta T'$ as a function of V_n for fixed $V_{sm} = 4$ cm/s at 1.8 K. The transitions to superfluid turbulence occur at $V_n = (0.75 \pm .25)$ and $V_n(4.25 \pm 0.25)$ cm/s. The trajectory for these data in the V_n-V_s plane is shown by the dashed line in Fig. 8.

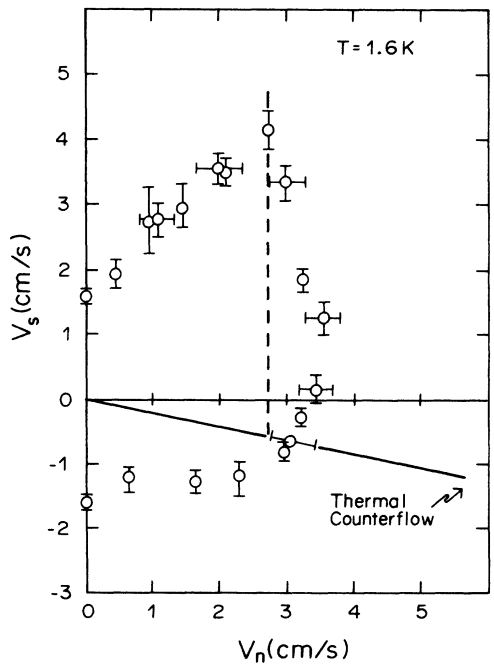

FIG. 7. The boundary of superfluid turbulence in the V_n-V_s plane at 1.6 K. The data points mark the transition between superfluid turbulence and laminar flow and fall on a critical line surrounding the origin. Points below the thermal counterflow line are from our previous results (Ref. 11).

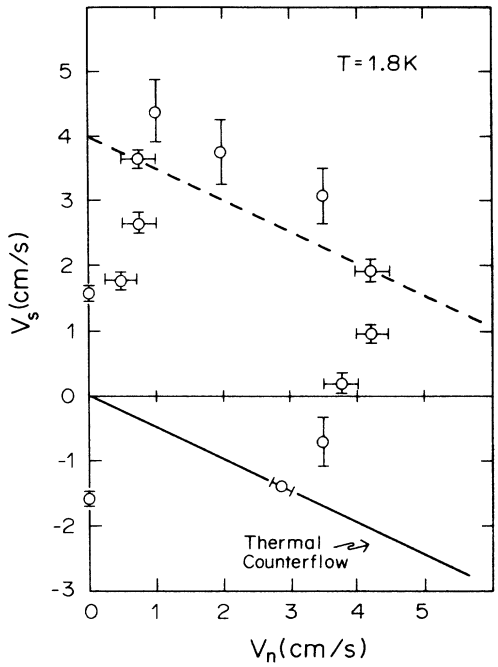

FIG. 8. The boundary of superfluid turbulence in the V_n-V_s plane at 1.8 K. The data points mark the transition between superfluid turbulence and laminar flow and fall on a critical line surrounding the origin. Points below the thermal counterflow line are from our previous results (Ref. 11).

ously,[11] while points above the line are the present extension of this earlier experiment. The solid circles in Fig. 6 are the data obtained from the roughened flow tube. No discernable difference was seen between the results for the roughened and smooth flow tube. The collection of boundary points in Figs. 6–8 may be taken to define a critical line in the V_n-V_s plane separating the region of superfluid turbulence from laminar vortex-free flow. Since the data from quadrants I and IV can be mapped into the physically equivalent quadrants II and III, the results show that the critical line is a closed curve about the origin.

The transition to superfluid turbulence in the V_n-V_s plane has also been observed by Marees *et al.*[8,9] at the University of Leiden. They used glass flow tubes of diameter $d=1.3\times10^{-2}$ cm and produced independent normal and superfluid velocities V_n and V_s using a combination of thermal counterflow and mass flow. Their experiment differs from ours however in the means of producing the superfluid mass flow V_{sm}. Instead of the FFTA (Fig. 1) which produces a constant value of V_{sm}, they essentially fill the large tube rising from the upper chamber and allow the helium to continuously drain through the superleak and flow tube into the reservoir. Their upper chamber is also held at the reservoir temperature T_1 so that the level difference Δz between the large tube and the reservoir is equal to the chemical potential drop $\Delta\mu$ across the flow tube. Data for Δz and $\Delta T'$ as a function of time are shown in Fig. 9 for a short tube ($l=14.5$ cm) and a very long one ($l=10.64$ m). The superfluid mass flow velocity V_{sm} at any time is obtained from the time derivative of Δz. The transition from superfluid turbulence to laminar flow is defined to occur when the chemical potential $\Delta\mu$ (proportional to Δz) first goes to zero. In the case of the short tube [Fig. 9(a)], the excess temperature difference $\Delta T'$ also goes to zero at the same time and velocity. The thermal resistance of the long tube is so large, however, that this is not the case as is shown in Fig. 9(b).

We compare our data for the boundary between superfluid turbulence and laminar flow with those[15] of Marees and van Beelen in Figs. 10–12. We have rendered all velocities dimensionless using the definitions

$$V_n^*=V_n d/4\pi\kappa\ , \tag{7}$$

$$V_s^*=V_s d/4\pi\kappa\ , \tag{8}$$

where κ is the quantum of circulation. In these figures the present data are shown as circles and the Leiden data as squares (open squares for the short tube, and solid squares for the long tube). The vertical dotted-dashed line in these figures represents the right-hand side of the

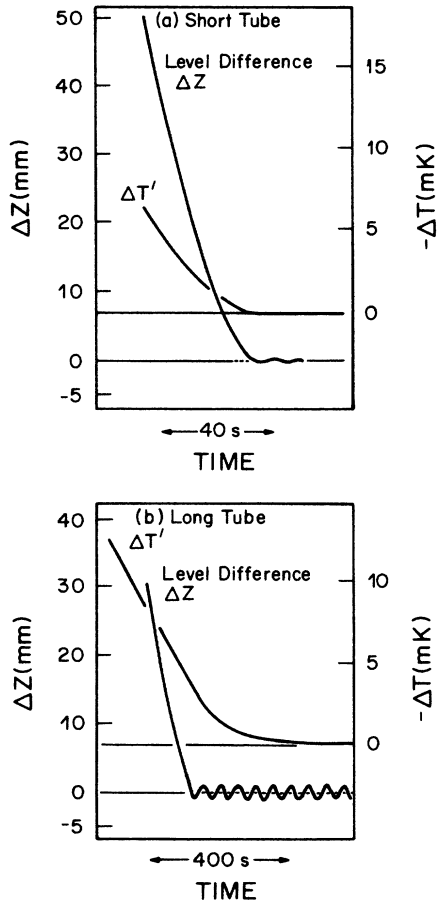

FIG. 9. In the experiments of Marees *et al.* (Refs. 8 and 9), the chemical potential difference $\Delta\mu$ (or the level difference ΔZ) and the excess temperature difference $\Delta T'$, decay in time as shown in these representative data for (a) a short tube and (b) a very long tube.

boundary between superfluid turbulence and laminar flow found in the Leiden experiments.

The best overall agreement between the two sets of data occurs at 1.6 K (Fig. 11). Here one can picture a smooth *critical line* in the V_n^*-V_s^* plane separating laminar flow from superfluid turbulence. As noted earlier, the data are duplicated in the second and third quadrants so the *critical line* forms a closed boundary about the origin. Clearly, the concept of a single critical velocity for the transition to superfluid turbulence is oversimplified. Critical velocities observed in pure superflow or in thermal counterflow actually represent the intersection of the experimental trajectory with the *critical line* in the V_n-V_s plane. Theories of the critical velocity will have to consider the stability of the superfluid turbulent state as a function of V_n and V_s together.

The agreement between the present data and the Leiden results is worse at 1.4 K (Fig. 10) and really terrible at 1.8 K (Fig. 12). The discrepancies could be due to the fact that the Leiden experiments are never truly in a steady state. Dynamic effects near the critical line could mask the actual transition. Marees and van Beelen consider such an effect to be plausible explanation for the discrepancies in their large tube data.[15] On the other hand, their thermal counterflow data point is obtained in a true steady-state measurement and differs from our result by a factor of 2 at 1.8 K. Flow tube length and surface roughness also do not seem to play a role. The data

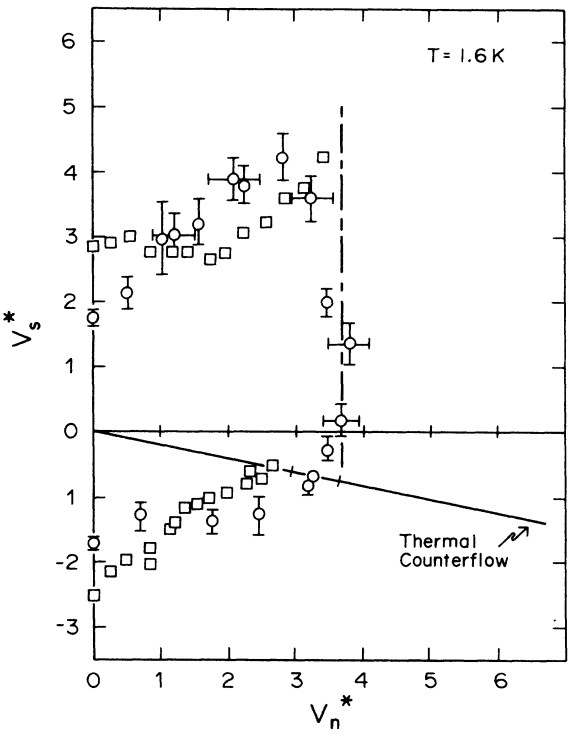

FIG. 11. The boundary of superfluid turbulence in the V_n^*-V_s^* plane at 1.6 K. The circles are our data (also shown in Fig. 7). The squares are the data of Marees *et al.* (Ref. 9) for the short tube. The vertical dotted-dashed line is the estimate in Ref. 9 for the right-hand limit of the boundary.

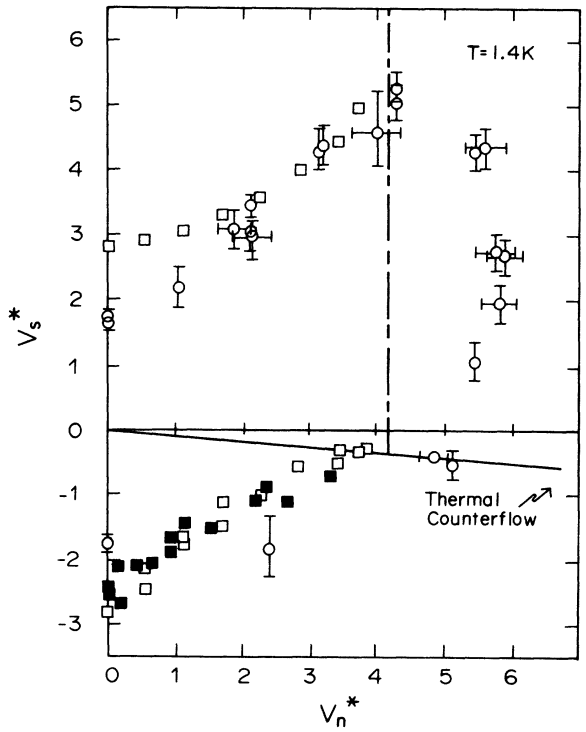

FIG. 10. The boundary of superfluid turbulence in the V_n^*-V_s^* plane at 1.4 K. The circles are our data (also shown in Fig. 6). The squares are the data of Marees *et al.* for the short tube (open symbols, Ref. 9) and the long tube (solid symbols, Ref. 8). The vertical dotted-dashed line is the estimate in Ref. 9 for the right-hand limit of the boundary.

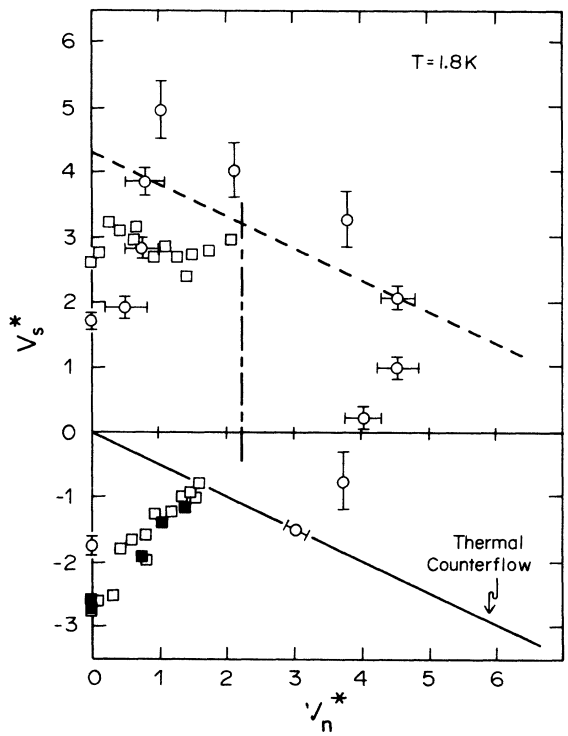

FIG. 12. The boundary of superfluid turbulence in the V_n^*-V_s^* plane at 1.8 K. The circles are our data (also shown in Fig. 8). The squares are the data of Marees *et al.* for the short tube (open symbols, Ref. 9) and the long tube (solid symbols, Ref. 8). The vertical dotted-dashed line is the estimate in Ref. 9 for the right-hand limit of the boundary.

are at slightly different temperatures,[16] but the correction for this difference should be minor. Yamaguchi *et al.*[17] have recently shown that the shape of the tube entrance can have a major influence on the critical velocity. Apparently, the stability of very low levels of superfluid turbulence is influenced by effects that are currently beyond experimental control. On the positive side, there is clear evidence for a *critical line* in the V_n-V_s plane, however poorly defined, separating superfluid turbulence from laminar flow.

A vast number of theories have been proposed for critical velocities in superfluid helium. Most of these give a critical value of a single velocity (V_n, V_s, or the relative velocity $V_n - V_s$) and are therefore inconsistent with the present data. One promising result has been recently obtained by Schwarz.[18] He considers the problem of remanent vortex lines pinned across the flow tube and subject to an imposed combined normal and superfluid flow. The pinning sites (imperfections on the flow tube surface) are taken to be on the order of 1/100 the tube size. The calculations lead to values of $V_{s,\mathrm{pin}}$ and $V_{n,\mathrm{pin}}$ at which these remanent vortex lines depin and are swept away. The collection of these depinning points forms a closed boundary about the origin in the V_n-V_s plane. Although this calculation bears a superficial resemblance to our data, and is important in that it includes V_s and V_n independently, it cannot be taken as the explanation for our observations. In the first place, we find no effect on the critical velocities when imperfections of the size used by Schwarz are introduced into the flow tube. Secondly, the calculated depinning velocities are an order of magnitude smaller than the observed critical velocities. Finally, and most important, the critical line in the V_n-V_s plane that we have described marks the boundary between superfluid turbulence and vortex-free laminar flow. There is no clear physical connection between this boundary and the condition for vortex depinning. Indeed, if the calculations are correct, then the remanent lines in the flow tube would all be depinned and swept away at velocities well below those defining the boundary for superfluid turbulence.

ACKNOWLEDGMENT

This work has been supported by the National Science Foundation, Low Temperature Physics Program under Grants Nos. DMR8218052 and DMR8619235.

[1]J. T. Tough, in *Progress in Low Temperature Physics*, edited by D. F. Brewer (North-Holland, Amsterdam, 1982), Vol. 8, p. 133.

[2]K. W. Schwarz, Phys. Rev. Lett. **49**, 283 (1982).

[3]R. A. Ashton, L. B. Opatowsky, and J. T. Tough, Phys. Rev. Lett. **46**, 658 (1981).

[4]G. van der Heijden, A. G. M. van der Boog, and H. C. Kramers, Physica (The Hague) **77**, 487 (1974).

[5]W. de Haas and H. van Beelen, Physica (The Hague) **83B**, 129 (1976).

[6]R. P. Slegtenhorst and H. van Beelen, Physica (The Hague) **90B**, 245 (1977).

[7]R. P. Slegtenhorst, G. Marees, and H. van Beelen, Physica (The Hague) **113B**, 341 (1982).

[8]G. Marees and H. van Beelen, Physica (The Hague) **133B**, 21 (1985).

[9]G. Marees, P. J. M. van der Slot, and H. van Beelen, Physica (The Hague) **144B**, 209 (1987).

[10]Marie L. Baehr and J. T. Tough, Phys. Rev. B **32**, 5632 (1985).

[11]Marie L. Baehr and J. T. Tough, Phys. Rev. Lett. **53**, 1669 (1984).

[12]Dow Chemical Company, Indianapolis, IN.

[13]A. C. Rose-Innes, *Low Temperature Techniques* (D. Van Nostrand, New York, 1964), p. 63.

[14]Model No. CG5N from Lake Shore Cryotronics, Westerville, OH.

[15]Some data were also obtained from glass tubes of 2.17×10^{-2} cm diameter. Since there is a substantial discrepancy between results obtained with long and short tubes of this diameter, we have not included these data in our discussion.

[16]The data of Refs. 8 and 9 were actually obtained at 1.41, 1.61, and 1.81 K.

[17]Minoru Yamaguchi, Yoshiko Fujii, Masayuki Kishida, and Masaki Nakamura, Proceedings of the 18th International Conference on Low Temperature Physics, LT-18, Kyoto, 1987 [Jpn. J. Appl. Phys. Suppl. 26-3 (1987)].

[18]K. W. Schwarz, Phys. Rev. B **31**, 5782 (1984).

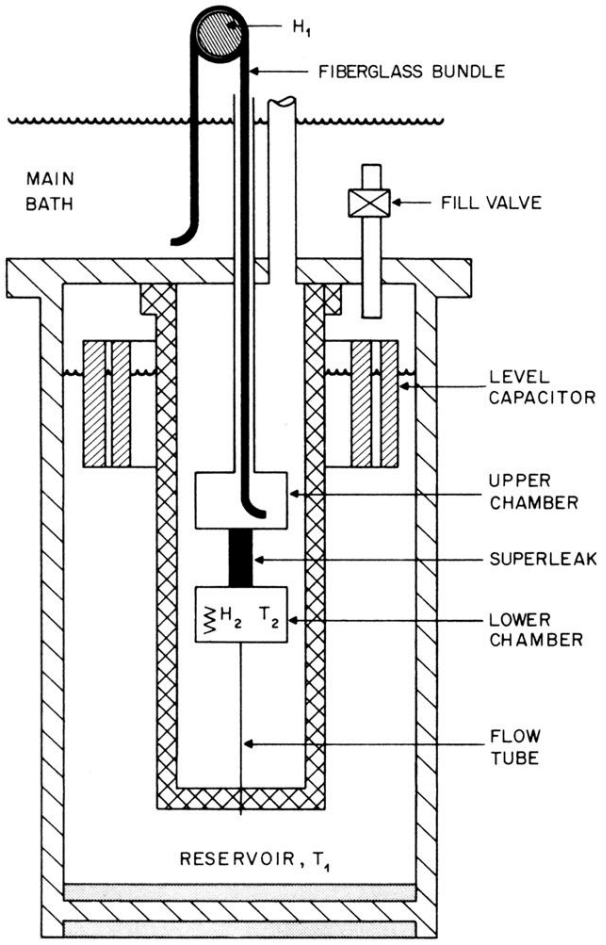

FIG. 1. Details of the experimental apparatus.